

RESEARCH

Open Access



# Selective gene expression profiling contributes to a better understanding of the molecular pathways underlying the histological changes observed after RHMVL

Janine Arlt<sup>1</sup>, Sebastian Vlaic<sup>2</sup>, Ronny Feuer<sup>3</sup>, Maria Thomas<sup>4</sup>, Utz Settmacher<sup>5</sup>, Uta Dahmen<sup>1\*</sup> and Olaf Dirsch<sup>6</sup>

## Abstract

**Background:** In previous studies, five vasoactive drugs were investigated for their effect on the recovery process after extended liver resection without observing relevant improvements. We hypothesized that an analysis of gene expression could help to identify potentially druggable pathways and could support the selection of promising drug candidates.

**Methods:** Liver samples obtained from rats after combined 70% partial hepatectomy and right median hepatic vein ligation ( $n = 6/\text{group}$ ) sacrificed at 0 h, 24 h, 48 h, and 7 days were selected for this study. Liver samples were collected from differentially perfused regions of the median lobe (obstruction-zone, border-zone, normal-zone). Gene expression profiling of marker genes regulating hepatic hemodynamics, vascular remodeling, and liver regeneration was performed with microfluidic chips. We used 3 technical replicates from each sample. Raw data were normalized using LEMming and differentially expressed genes were identified using LIMMA.

**Results:** The strongest differences were found in obstruction-zone at 24 h and 48 h postoperatively compared to all other groups. mRNA expression of marker genes from hepatic hemodynamics pathways (iNOS, Ptg2, Edn1) was most upregulated.

**Conclusion:** These upregulated genes suggest a strong vasoconstrictive effect promoting arterial hypoperfusion in the obstruction-zone. Reducing iNOS expression using selective iNOS inhibitors seems to be a promising approach to promote vasodilation and liver regeneration.

**Keywords:** Liver resection, Portal hypertension, Gene expression, Vasoactive drug

## Introduction

Extended liver resection leads to a reduction of functional liver mass beyond the surgical loss. Extended liver resection leads to portal hypertension and arterial

hypoperfusion of the liver remnant [1, 2]. Furthermore, extended liver resection requires transection of the middle hepatic vein and leads to focal outflow obstruction. Together, arterial hypoperfusion and focal outflow obstruction compromise the perfusion of the liver remnant. This leads to pericentral necrosis of the undrained territories and subsequently to an additional loss of functional liver mass [3–5]. The additional loss of functional liver mass after extended liver resection may lead

\*Correspondence: Uta.Dahmen@med.uni-jena.de

<sup>1</sup> Experimental Transplantation Surgery, Department of General, Visceral and Vascular Surgery, Jena University Hospital, Drackendorfer Str. 1, 07747 Jena, Germany

Full list of author information is available at the end of the article



to hepatic insufficiency and ultimately cause the death of the patient [6–9].

Portal hypertension after extended liver resection can be treated by operative interventions in clinical practice. Additional procedures such as splenectomy are performed to reduce the surgically induced portal hypertension. However, performing an additional procedure may increase the overall risk for complications [10–14].

Portal hypertension, especially in chronic cirrhotic liver disease, can be treated by drug administration. Drugs acting as vasodilators such as non-selective  $\beta$ -blockers (propranolol, carvedilol), nitric oxide (NO) donors (isosorbide dinitrate, isosorbide-5-mononitrate), or drugs to decrease portal venous blood flow (terlipressin, octreotide) are administered for the treatment of portal hypertension [15–18]. Pharmacological treatment of portal hypertension after extended liver resection may prevent the complications induced by additional operative interventions and should be further investigated.

Liver regeneration after extended liver resection is a complex process. The complexity is due to the simultaneous activation of interwoven signaling mechanism. On one hand, liver resection leads to the activation of liver regeneration to restore the functional liver mass. On the other hand, the imbalance of hepatic hemodynamics leads to the activation of vasoactive mechanisms and vascular remodeling to restore hepatic venous drainage [4, 19–25].

The interwoven signaling mechanisms can be grouped as follows:

*Hepatic hemodynamics* Regulation of hepatic hemodynamics is controlled by different vasoactive mechanisms. Vasoactive mechanisms are activated by portal hypertension and arterial hypoperfusion. The main mechanisms are the adenosine-based “Hepatic arterial buffer response” (HABR), NO pathway, the endothelin pathway, and the arachidonic acid pathway [20, 22, 23].

*Vascular remodeling* Focal outflow obstruction induces a vascular remodeling process. The liver restores hepatic venous drainage through the formation of sinusoidal vascular canals in the border zone (BZ) between the outflow obstruction zone (OZ) and the normal zone (NZ) [3, 24, 26].

*Liver regeneration* Liver regeneration is induced in both, the drained NZ and the OZ, by the loss of liver mass and the resulting portal hyperperfusion and parenchymal necrosis. The essential factors involved in liver regeneration are encompassed by three types: cell cycle-associated marker genes, hepatocyte growth factors, and cytokines. The signaling mechanisms of liver regeneration have been

described in detail, e.g., by Fausto et al. (2006), Michalopoulos (2007), and Riddiough et al. (2021) [19, 21, 25].

First insights into the spontaneous recovery process of outflow obstruction after extended liver resection were previously obtained in a newly developed surgical model in rats combining focal hepatic outflow obstruction (FHO) and extended liver resection. Dirsch et al. (2008) and Huang et al. (2014) used this model to investigate liver recovery after extended liver resection. They induced FHO by right median hepatic vein ligation (RMHVL) performed in the same operation as the partial hepatectomy (PHx). They showed that revascularization via the formation of sinusoidal canals as well as liver mass restoration was completed within a week after the surgical intervention. During the postoperative recovery and regeneration phase, confluent pericentral necrosis was resorbed and replaced by proliferating hepatocytes [3, 26].

Huang et al. (2011) investigated the role of arterial blood supply by comparing the spontaneous recovery from hepatic outflow obstruction in a non-arterialized versus arterialized partial liver transplantation model. He demonstrated that the lack of hepatic arterial perfusion determined the extent of hepatic necrosis in OZ [4].

Furthermore, Huang et al. (2014) investigated the effect of modulating hepatic arterial perfusion by influencing the NO pathway in the surgical model of extended liver resection with FHO [26]. The molecular compound NO increases the hepatic arterial flow by arterial vasodilation [26–28]. However, the application of molsidomine, a NO donor, did not show the expected beneficial effect. In contrast, the application of N( $\omega$ )-nitro-L-arginine methyl ester (L-NAME), a competitive NO synthase (NOS) inhibitor, reduced hepatic arterial flow, increased parenchymal necrosis, and delayed spontaneous recovery, as expected [26].

In a subsequent study, five clinically established vasoactive drugs were investigated for their ability to improve hepatic perfusion in this situation. The selection was guided by a thorough knowledge-based literature work-up of more than 20 drug classes addressing different molecular pathways such as NO pathway, arachidonic acid pathway, and endothelin pathway. However, despite a modulatory effect on hepatic hemodynamics, no relevant improvement of hepatic damage was observed [9, 29].

We hypothesized that an analysis of gene expression could help to identify potentially druggable pathways and could support the selection of promising drug candidates. Therefore, this study aimed to identify regulated signaling pathways based on selected marker genes.

Due to the numerous signal transduction pathways involved in the complex recovery process, only a selection of marker genes representing the different mechanisms was analyzed using quantitative high-throughput reverse transcription PCR (RT-qPCR). The selected genes are involved in regulatory processes underlying the regulation of hepatic hemodynamics, vascular remodeling, and liver regeneration. The simultaneous investigation of the respective gene expression levels allows for a hypothesis-driven analysis of signaling pathways in contrast to a transcriptome analysis.

We compared gene expression in healthy control animals and animals subjected to extended liver resection with RMHVL at different time points and in the three different zones. The gene expression analysis revealed highly regulated significantly differentially expressed potential marker genes and thereby the most affected pathways.

## Materials and methods

### Sample generation

For this gene expression study, we used a set of previously generated liver samples [26]. Male inbred Lewis (Lewis/HanTMHsd) rats (250–350 g, Central Animal Laboratory, University Hospital Essen, Germany) had been subjected to RMHVL in combination with 70% PHx. The left lateral lobe, the left median lobe, the superior plus inferior caudate lobes, and the right superior plus inferior lobes were resected, leading to an estimated 70% reduction of liver mass. Liver tissue samples were taken from the obstructed territory of the RMHV (OZ), normal zone (NZ), and border zone between OZ and NZ (BZ) and were snap-frozen immediately after surgery and stored in liquid nitrogen until used. Samples from 6 animals were taken at each observation time (0 h, 24 h, 48 h, 7days).

All procedures, experiments, and housing of the animals were carried out according to current German regulations and guidelines for animal welfare and to international principles of laboratory animal care,

following the ARRIVE Guidelines Checklist as well. Ethics committee of Thüringer Landesamt für Verbraucherschutz, Thuringia, Germany, approved this animal study. The protocols were approved by the Thüringer Landesamt für Verbraucherschutz, Thuringia, Germany (Approval-Number: 02–023/14).

### Selection of marker genes for quantitative high-throughput RT-qPCR analysis

*First*, we performed a thorough literature review to identify the relevant biological mechanisms involved in regulatory processes underlying the regulation of hepatic hemodynamics, vascular remodeling, and liver regeneration.

*Second*, we selected 3–7 genes for each pathway, which resulted in a total of 37 marker genes. The following marker genes from the key signal transduction pathways (Table 1) were selected for the analysis:

For regulation of hepatic hemodynamics, we selected 16 marker genes from four vasoactive mechanisms. The selected marker genes of these four mechanisms were as follows: The NO pathway was represented by the marker genes eNOS, iNOS, nNOS, and Gucy1a2, the arachidonic acid pathway by the marker genes Pla2g4a, Ptgs1, Ptgs2, Ptgis, Tbxas1, Tbxas2r, the endothelin pathway by the marker genes Edn1, ET-R<sub>A</sub>, and ET-R<sub>B</sub>, and the adenosine-based HADR was represented by the marker genes Adora1, Adora2a, and Adora3 (Fig. 1).

For vascular remodeling, we considered the following 8 genes: CAV1, Vegfa, Vegfb, Icam1, Pecam1, Prdx1, vWF, and Lamc2 as marker genes.

For liver regeneration, we selected 13 marker genes including cell cycle-associated genes, hepatocyte growth factors, and cytokines. Cell cycle-associated marker genes were represented by PCNA and Tyms. The following growth factors and receptors were included: Egf, Egfr, Egr1, Hgf, and Met. We selected six cytokines (IL10, IL1b, IL6, Mif, Tgfb1, and Tnf) relevant for liver regeneration.

**Table 1** List of selected marker genes\*

Mechanisms	Pathways	Genes	References (e.g.)
Vasoactive pathways	NO pathway	eNOS, iNOS, nNOS, Gucy1a2	[22], [28], [35]
	Arachidonic acid pathway	PLA2G4A, COX1, COX2, PGIS, TXS, Tbxas2r	[27], [36]
	Endothelin pathway	Edn1, ET-R <sub>A</sub> , ET-R <sub>B</sub>	[27], [36], [37]
	Hepatic arterial buffer response <sup>a</sup>	Adora1, Adora2a, Adora3	[20], [23]
Vascular remodeling		CAV1, Icam1, Pecam1 Prdx1, vWF, Lamc2, Vegfa, Vegfb	[24], [37–39]
Liver regeneration	Liver cell proliferation	PCNA, Tyms	[40], [41]
	Liver cell growth factors	Egf, Egfr, Egr1, Hgf, Met	[19], [21, 25]
	Cytokines	IL10, IL1b, IL6, Mif, Tgfb1, Tnf	[22], [25], [36], [37]

\* List of selected marker genes for each mechanism and pathway based on selected references

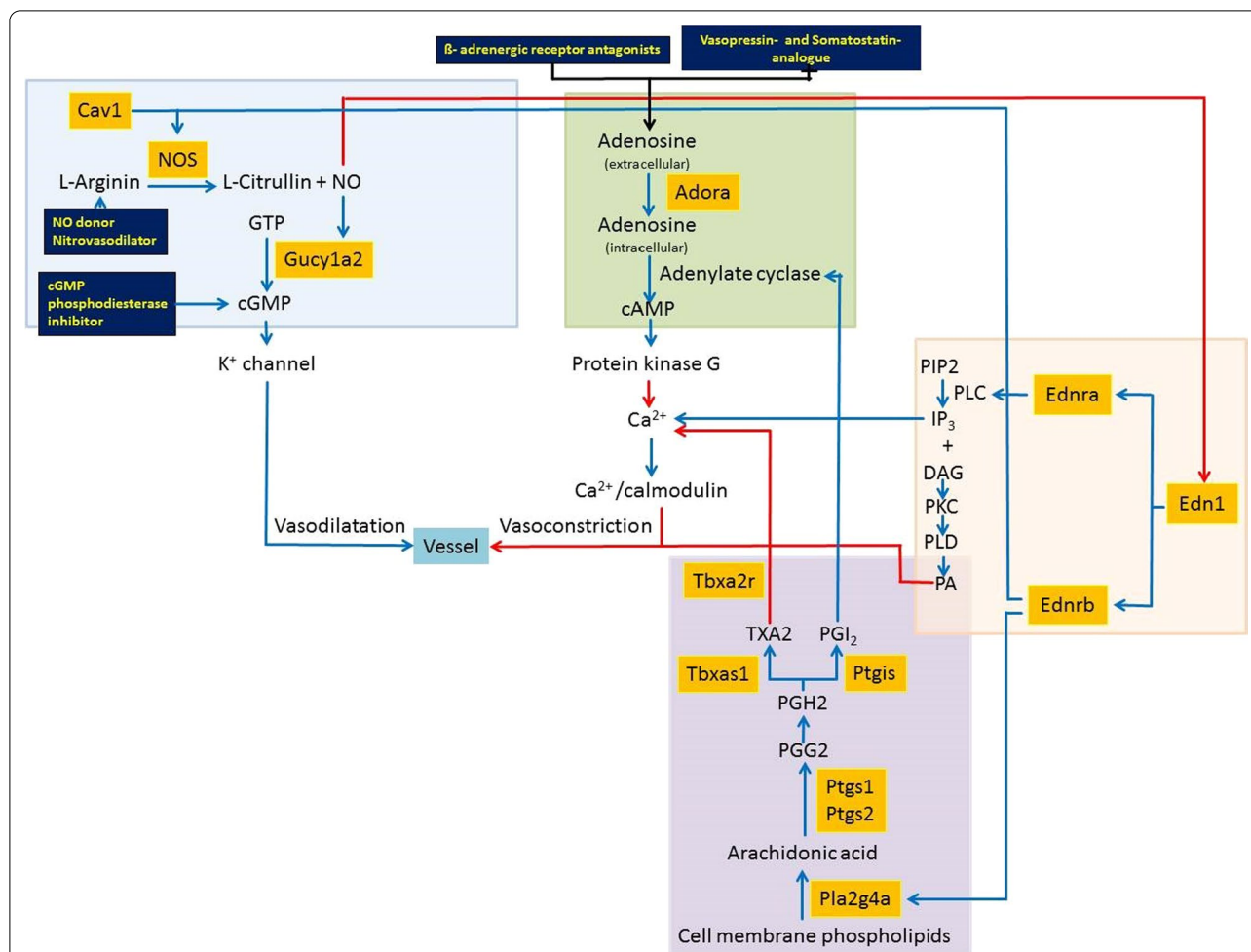


**Fig. 1** Diagram of different vasoactive molecular pathways involved in the regulation of hepatic hemodynamics. List of interactions between pathways: blue arrows—enhancing effect, red arrows—inhibitory effect; dark blue tiles: interrelated drug classes; yellow text—drug classes with substance investigated in previous studies; orange box—investigated genes. By courtesy of Springer Nature: Modified figure of previously published figure in Arlt et al. (2017) [29]. List of abbreviations: Adora, Adenosine receptor; Ca<sup>2+</sup>- Calcium; cAMP, cyclic adenosine monophosphate; cGMP, cyclic guanosine monophosphate; DAG Diacylglycerol; Edn1-Endothelin 1; Ednra, Endothelin receptor type A; nEdra, Endothelin receptor type B 1/2; GTP, Guanosine triphosphate; GucY1a2- Guanylate cyclase soluble subunit alpha-2; IP<sub>3</sub>, Inositol 1,4,5-trisphosphate; K<sup>+</sup> -Potassium; NO, Nitric oxide; NOS, Nitric oxide synthases; PA- Phosphatidic acid; PGH<sub>2</sub>, Prostaglandin H<sub>2</sub>; PGI<sub>2</sub>, Prostacyclin; Ptgis -Prostacyclin synthase; PIP<sub>2</sub>, Phosphatidylinositol 4,5-bisphosphate; PKC- Protein kinase C; PLC -Phospholipase C; PLD, Phospholipase D; Ptgis 1/2 -Cyclooxygenase-1/2; TXA<sub>2</sub>- thromboxane A<sub>2</sub>; Tbx2r -Thromboxane A<sub>2</sub> Receptor; Tbx1- Thromboxane synthase

The remaining 59 slots were used for other genes which were investigated in other studies in our lab.

**Determination of gene expression values using quantitative high-throughput RT-qPCR analysis**

The mRNA was isolated from the frozen liver tissue samples using the Qiagen RNeasy Mini Kit (Valencia, CA). The mRNA quantity was measured using Nanodrop (Thermo Scientific, Waltham, MA). The RNA integrity number (RIN) was checked using Agilent 2100 Bioanalyzer (Agilent Technologies, Santa Clara, CA) and was above 8.5 for all samples. cDNA synthesis was performed

with 2µL of 50 ng/µL total RNA, 1µL of 10 × TaqMan RT Buffer, 2.2µL 25 mM MgCl<sub>2</sub>, 2µL of 2.5 nM dNTP-Mix, 0.5µL of 50 µM random hexamers, 0.2µL of RNase Inhibitor, 0.25µL of 50 U/µL Multiscribe reverse transcriptase, and 1.85µL RNase-free water. All reagents were purchased from Applied Biosystems (TaqMan Reverse Transcription Reagents: N808-0234). The reaction mixtures were mixed with the RNA and incubated at 25 °C for 10 min, at 48 °C for 30 min, and then at 95 °C for 5 min. The generated cDNAs were run on a 96.96 microfluidic Dynamic Array™ IFC (Fluidigm Corporation, CA, USA), using a BioMark Instrument 76 (GE96X96 Standard

v1.pcl – protocol file) and analyzed with Real-Time PCR 182 Analysis Software in the BIOMARK instrument (Fluidigm Corporation, CA, USA). From the cDNA samples, 3 technical replicates were used for the amplification step. Gene-specific primers were purchased from Life Technologies (Darmstadt, Germany). A listing of all primers is provided in the Additional file 1: (S1).

#### Normalization of gene expression values using the linear (L) error (E) model (M)—ming method (LEMming)

The analysis of qPCR raw data was performed using the LEMming method for the Fluidigm platform [30]. The Fluidigm platform with its parallel qPCR measurements implicates an experimental design that allows the estimation and exclusion of technical errors and thus a data normalization independent from reference genes. Thus, normalization using LEMming is based on a linear model including a number of effect variables that are estimated in the following order:

1. Probe error per array ( $\varepsilon_{P:A}$ ).
2. Systematic batch effects ( $\varepsilon_S$ ).
3. Treatment/tissue effect ( $\Delta_T$ ).
4. Sample error ( $\varepsilon_S$ ).
5. Treatment effect per gene ( $\Delta_{T:G}$ ).

According to the linear model shown in Eq. 1, each measurement  $Y$  of a gene is a composition of these effects.

$$Y = \varepsilon_{P:A} + \varepsilon_S + \Delta_T + \Delta_{T:G} + \varepsilon \quad (1)$$

The variable  $\varepsilon$  is called residual and describes biological variance and non-systematic technical errors. The sum of  $\Delta_T + \Delta_{T:G}$  is used to calculate the fold change in comparison to a control condition.

Pre-processed LEMming cycle threshold (CT)-values were then transformed into  $2^{\Delta CT}$  expression values and normalized to the untreated control samples. The normalization using LEMming and further computational analyzes were performed using R [31]. The list of all gene expression data is included in the Additional file 2: (S2).

#### Clustering of sample groups based on gene expression data

The time-dependent expression of genes across tissue zones was analyzed using hierarchical clustering and principal component analysis (PCA). The hierarchical clustering was used to group samples according to gene expression profiles over time and all three zones (NZ, BZ, and OZ). The gene expression values were graphically represented in the heatmap. The samples were sorted according to the correlations of their gene expression profiles and their clustering presented in a dendrogram.

The hierarchical clustering was visualized using the “gplots” package for R [32] (Fig. 2).

Additionally, PCA was used to visually group samples based on gene expression profiles in a scatter plot. PCA is a multivariate technique that reduces the high dimensionality of the data. A multivariate dataset is visualized as a set of coordinates in high-dimensional data space (1 axis per gene corresponding to 37 dimensions in this study). Using this method, a smaller set of coordinates was determined in a retransformed multi-dimensional space. The reduction of coordinates was done by determining a new eigenvector that captures maximum variance in the original high-dimensional data. Based on the reduction of dimensions and the visualization of data with the highest variance, patterns within the data were recognized [33] (Fig. 3A).

#### Identification and clustering of differentially expressed genes (DEGs) using linear models for microarray data (LIMMA)

LIMMA was used for the identification of DEGs [34]. Identification of DEGs over time (0, 24, 48, and 168 h post-op) compared to control (untreated) was performed for each of the tissue zones (NZ, BZ, and OZ) independently. Differential expression was assessed based on a Benjamini–Hochberg corrected  $p$ -value  $< 0.05$  in combination with a threefold change in expression. The list of all gene expression data is included in the Additional file 2: (S2).

#### Clustering of DEGs

The zonal distribution of DEGs was investigated using a Venn diagram. The Venn diagram visualized the numeric distribution of DEGs within the three tissue zones (NZ, BZ, and OZ).

The three tissue zones were visualized using circles. The numbers indicated in the circles correspond to the number of DEGs in the respective tissue zones. The number of DEGs that were differentially expressed in more than one tissue zone was indicated in the overlapping circles (Fig. 3B).

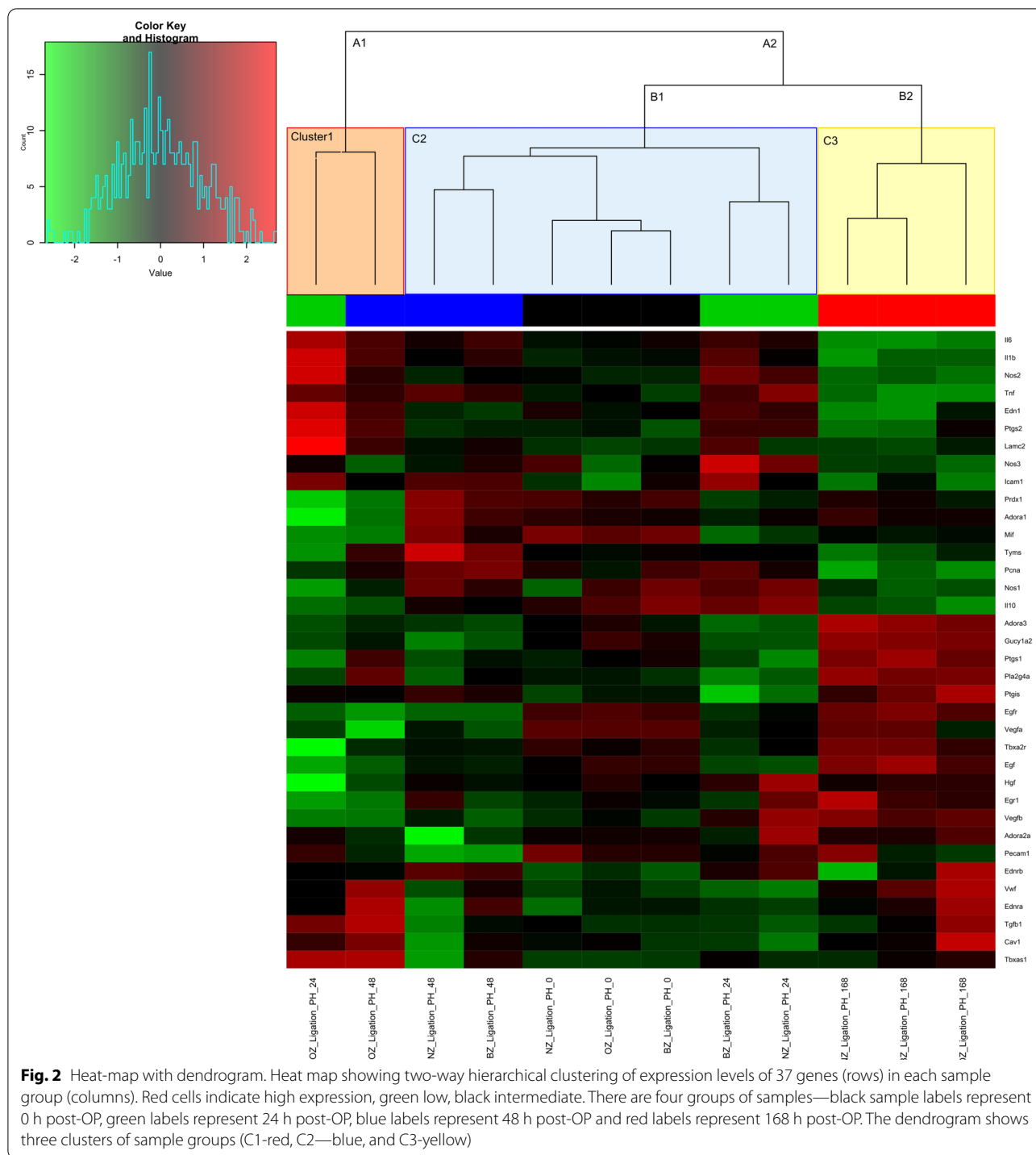
## Results

### Bioinformatic analysis

#### Clustering of data using hierarchical clustering and PCA

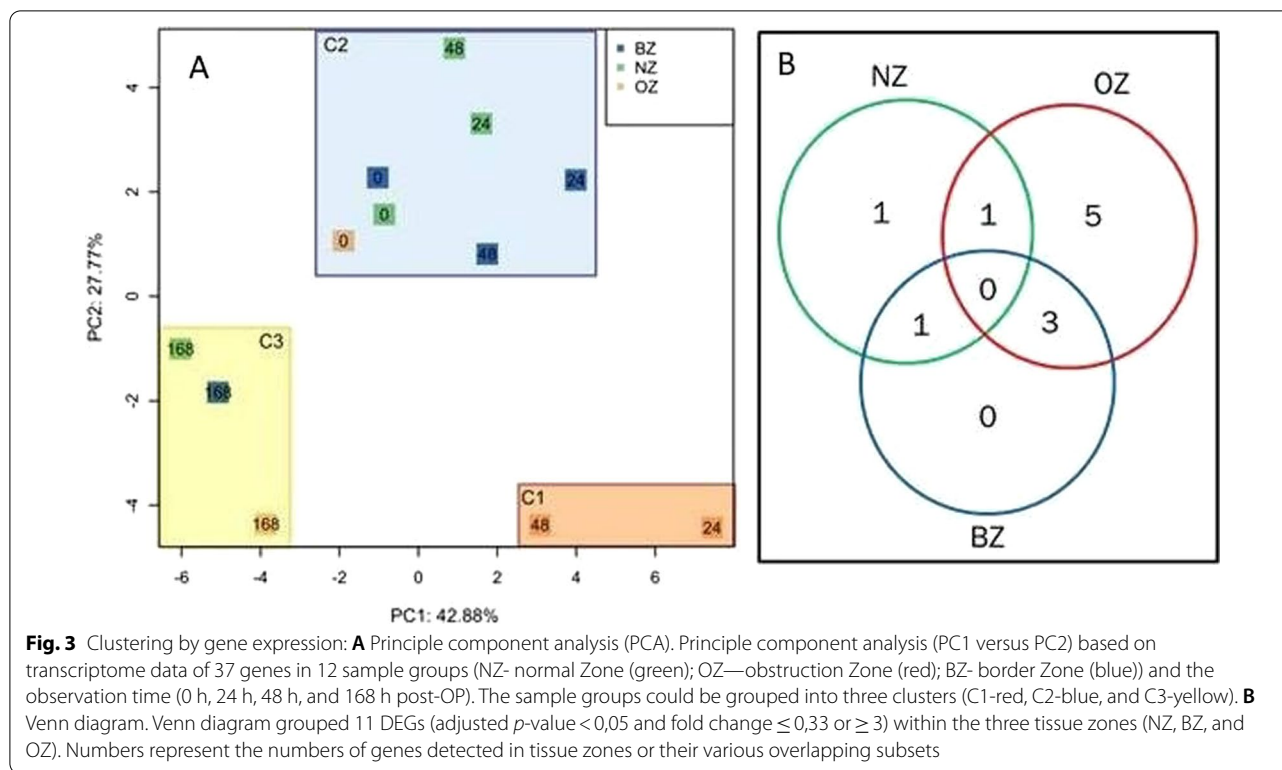
Two independent clustering algorithms revealed the same grouping of samples.

Hierarchical clustering with dendrogram grouped the samples based on the similarity of their gene expression profile (Fig. 2). As shown in the dendrogram, the analysis resulted in two main clusters (A1 and A2). The separation of the samples in the main clusters A1 and A2 visualized the strong differences in gene expression profiles



between OZ samples at 24 h and 48 h (C1) and all other groups (A2). In contrast to A1 containing the only C1, cluster A2 was further divided into 2 large sub-clusters. Subcluster B1 contained all remaining samples, except the samples obtained at the end of the observation period of 168 h (C2), which formed a separate cluster (B2—C3).

By performing PCA, we found the first two principal components (PCs) to account for 70, 7% of the original biological variability in the dataset (PC1: 42,88%, PC2: 27,77%) (Fig. 3A) and three clearly separated clusters corresponding to the dendrogram. Cluster 1 (C1) enclosed the 24 h and 48 h samples from the OZ, C2 contained all



0 h samples as well as 24 h and 48 h samples from NZ and BZ and last but not least, C3 included all 168 h samples.

Hierarchical clustering and PCA showed that the greatest differences in gene expression occur at the time points 24 h and 48 h. For this reason, we concentrated on these two time points with the greatest changes for further evaluation.

#### Visualization of data using a venn diagram

Using the LIMMA analysis, we identified significantly DEGs (adjusted  $p$ -value < 0,05 and fold change  $\leq 0,33$  or  $\geq 3$ ) at 24 h and 48 h postoperatively compared to control (untreated). Using this cutoff, we identified 11 DEGs (Table 2). Complete results are shown in Additional file 2: data (S2).

We visualized the number of differentially expressed marker genes according to the distribution in the different tissue zones in a Venn diagram (Fig. 3B). However, we observed a striking imbalance between the numbers of DEGs in OZ compared to the other two zones. The diagram depicts that five DEGs were found only in the OZ, whereas in the NZ and BZ only one gene and no gene was differentially expressed respectively. This pattern of distribution correlates well with the patterns revealed by the dendrogram and PCA, in which the OZ also differed significantly from the other zones.

#### Analysis of DEGs in respect to the three perfusion zones (OZ, BZ, NZ) in the liver

**OZ** The gene analysis showed that 7 genes were upregulated, and 2 genes were downregulated in OZ at 24 h and 48 h post-OP compared to control (untreated). Among the DEGs, iNOS (73-fold), Lamc2 (15-fold), Ptgs2 (tenfold), and Edn1 (eightfold) emerged as the most upregulated genes at 24 h postoperatively (Table 2). These genes are involved in three hepatic hemodynamic regulatory mechanisms: NO pathway (iNOS), arachidonic acid pathway (Ptgs2), and endothelin pathway (Edn1). These upregulated genes are also known to be involved in pro-inflammatory responses [42, 43]. In particular, iNOS was strikingly more upregulated (70-fold) than the marker genes of other hepatic hemodynamic pathways. This finding suggests that the NO pathway could potentially be targeted for the reduction of damage from outflow obstruction after extended liver resection.

Another highly upregulated gene in OZ was Lamc2 (15-fold), a marker gene for vascular remodeling and a component of the basal lamina.

The following genes: iNOS (11-fold), Ptgs2 (threefold), and Lamc2 (threefold) were also over-expressed in BZ (Table 2).

In OZ, the most downregulated genes were EGF (0,twofold) and HGF (0,threefold) (Table 2). These genes encode growth factors relevant for liver regeneration.

**Table 2** Differentially expressed genes (expressed as fold-change) compared to the control group

Mechanisms	Genes	NZ		BZ		OZ	
		24h	48h	24h	48h	24h	48h
hepatic hemodynamics	nNOS	6*	5*	6	3	0,7	2
	iNOS	2	0,4	11*	1	73*	2
	Cav1	0,7	0,8	1	2	2	3*
	Ptgs2	3	0,7	3*	1	10*	2
	Tbxas1	1	0,9	2	2	4*	4*
	Edn1	2	1	3	1	8*	3
	Ednra	2	1	2	3	2	4*
vascular remodeling	Lamc2	1	1	3*	2	15*	4*
liver regeneration	Tyms	2	6*	2	4*	0,6	3
	Hgf	3*	2	2	1	0,3*	0,9
	Egf	0,5	0,8	0,5	0,8	0,2*	0,4

\* adjusted  $p$ -value < 0,05; color code to highlight fold change  $\leq 0,33$  (blue) or  $\geq 3$  (light red),  $\geq 5$  (red),  $\geq 10$  (bright red), compared to control (untreated)

Downregulation of gene expression corresponded to the inhibition of proliferation observed in histology at this observation time point [26].

**NZ** In contrast, our analysis revealed that only 3 genes, nNOS, Tyms and HGF, were moderately upregulated in NZ at 24 h and 48 h post-OP (3- to sixfold) compared to control (untreated) (Table 2). Overexpression of nNOS suggests an effect on vasodilatation which corresponded to the obvious sinusoidal dilatation occurring in the NZ at this time point. Overexpression of HGF and Tyms did fit well to the regenerative response of hepatocytes in the NZ. The cell cycle-associated marker Tyms was also moderately overexpressed (fourfold) in the BZ, also corresponding to the observed proliferative response (Table 2).

## Discussion

### Justification of selective gene expression profiling

In this study, we used selective gene expression profiling analysis to investigate a complex biological process. Quantitative high-throughput RT-qPCR by 96.96 microfluidic Dynamic Array™ from Fluidigm enables the investigation of many samples. In our study, we examined 6 rats (biological replicates) at each observation time point 0 h, 24 h, 48 h, and 7days. We analyzed three perfused regions (NZ, BZ, OZ) per rat liver. We applied 3 technical replicates of all samples to the "Dynamic Array™ IFC" Fluidigm chip. This resulted in a total number of 216 samples. Hence, differential gene expression analysis which is used for whole-genome gene expression profiling is far too expensive for that many samples. Based on well-known signaling mechanisms interwoven in hepatic

hemodynamics, vascular remodeling, and liver regeneration we focused our analysis on 37 genes with specific interest for this scientific question.

### Identification of molecular pathways underlying the histological findings

One of the factors decisive for the outcome is the prevention of arterial hypoperfusion and subsequently the prevention of hepatic necrosis. Since, as reported before, all previously selected drugs: molsidomine, isosorbide-5-mononitrate, sildenafil, carvedilol, terlipressin, and octreotide, did not affect hepatic hemodynamics, we wanted to identify key regulatory mechanisms using selective gene profiling.

First, we confirmed the suitability of our strategy. Therefore, we first compared the expression of selected marker genes with the expected corresponding histological findings in terms of liver regeneration and vascular remodeling. Second, we analyzed the results of the expression level of the marker genes governing hepatic hemodynamics.

The bioinformatic analysis (hierarchical clustering and PCA) revealed that differences in gene expression were most prominent at 24 h and 48 h and occurred predominantly in the OZ (Venn diagram) compared to the other time points and zones (Fig. 2, 3). These findings corresponded to the previous histological observations showing that the most obvious changes occurred indeed in the OZ at this time point [26].

Gene expression analysis showed that the liver regeneration marker (Tyms) was the most upregulated gene in NZ and BZ, corresponding to the pronounced hepatocyte

proliferation. In contrast, other markers of liver regeneration (HGF and EGF) were markedly downregulated in OZ at 24 h corresponding to the absence of hepatocyte proliferation in this region. Similarly, we observed that upregulation of the vascular remodeling marker *Lamc2* corresponded well with the formation of vascular canals in OZ and BZ of these animals as previously described by Huang et al. (2014) [26]. These findings suggest that the selected marker genes were indeed indicative of the histological alterations.

Regulation of hepatic hemodynamics is based on four intermingled key signaling pathways: Adenosine-based HABR, NO pathway, arachidonic acid pathway, and endothelin pathway.

#### **Adenosine-based HABR**

HABR leads to vasodilatation via the regulation of the adenosine concentration in the "Space of Mall". The adenosine in the "Space of Mall" binds to the adenosine receptors of the hepatic arterial vessel wall. If the adenosine receptors are activated, arterial vascular dilatation occurs.

We investigated the expression of adenosine receptor genes: *Adora1*, *Adora2a*, and *Adora3* (Fig. 1).

All three adenosine receptor genes were not differentially expressed at 24 h or 48 h after the operation. This result corresponds to the observations of the studies by Dold et al. (2015) and Audebert et al. (2017) [44, 45]. Dold et al. (2015) observed that portal hyperperfusion after 70% and 90% hepatectomy did not induce a HABR [44]. Audebert et al. (2017) investigated hemodynamic changes during partial liver resection and created a computational model of hepatic hemodynamics. They observed a 75% decrease in hepatic arterial blood flow during surgery [45]. Based on their simulation, they showed that this 75% decrease in hepatic arterial flow can be explained by the increase in resistance induced by the surgical procedure itself.

These and our studies suggest that the HABR is not necessarily required for the regulation of liver perfusion in this situation. Thus, targeting the HABR does not seem to be a suitable strategy to influence liver perfusion after extended liver resection.

#### **NO pathway**

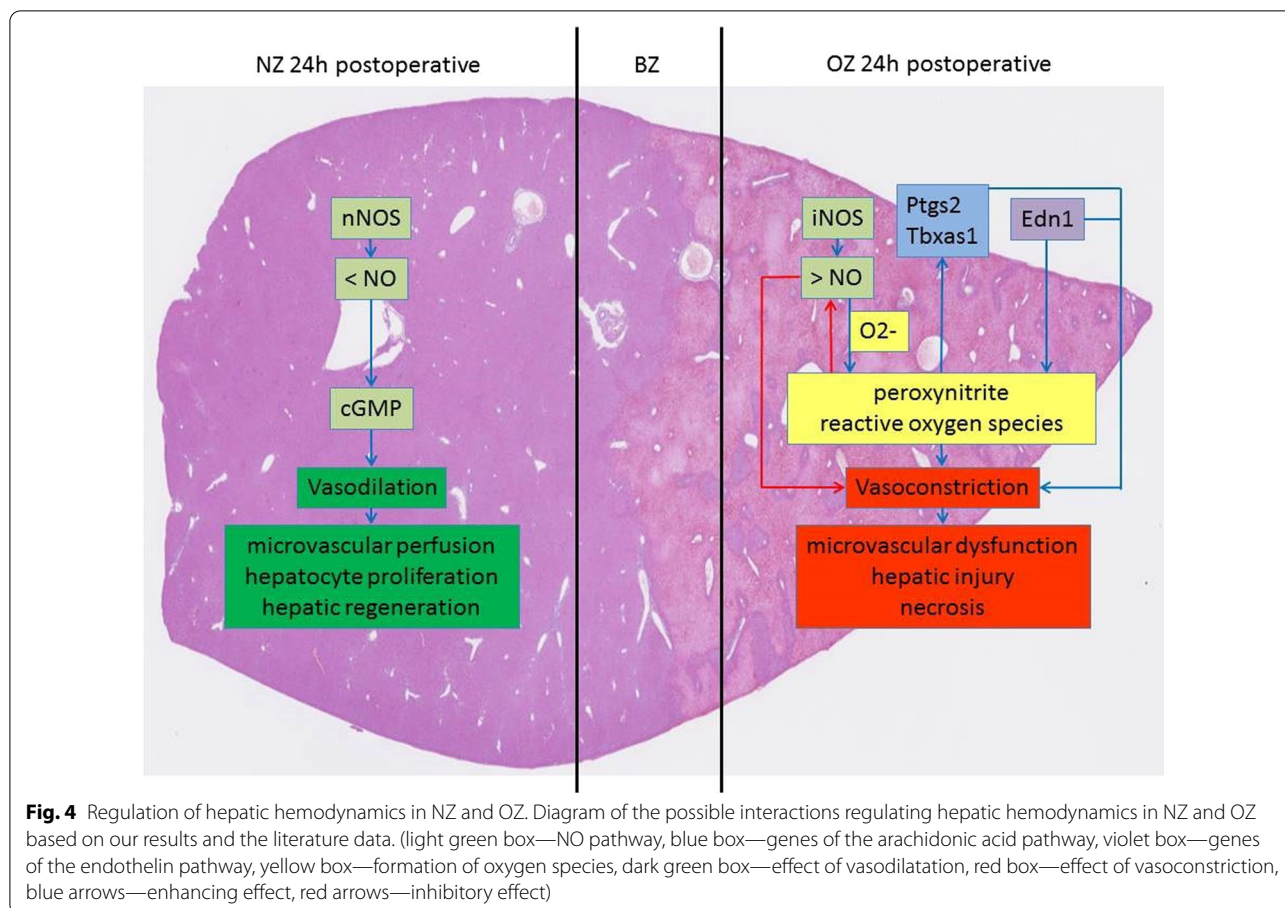
NO pathway leads to vasodilatation via conversion of L-arginine by activation of guanylate cyclase (*Gucy1a2*) (Fig. 1). NOS catalyzes the production of NO from L-arginine. eNOS, iNOS, and nNOS are three isoforms of NOS. NO increases the activity of guanylate cyclase, thereby increasing the concentration of cyclic guanosine monophosphate (cGMP), which in return leads to vasodilatation.

We selected 4 genes as marker genes from the NO pathway: eNOS, iNOS, nNOS, and *Gucy1a2* (Fig. 1).

Both eNOS and *Gucy1a2* were not differentially expressed, neither at 24 h nor at 48 h after the operation.

In contrast, nNOS mRNA-expression increased by six-fold, but only in NZ. nNOS is constitutively expressed and leads to the generation of only small amounts of NO [46]. nNOS increases vascular cGMP production and promotes vasodilatation [47] (Fig. 4). However, NO is a double-edged sword. Low levels of NO lead to vasodilatation such as the NO release by nNOS [48]. In contrast, high levels of NO promote vasoconstriction, which might contribute to microvascular dysfunction and hepatic injury [49, 50] (Fig. 4). iNOS is the inducible isoform of NOS and generates 1000-fold larger quantities of NO than nNOS [27]. In our study, iNOS was the highest up-regulated gene (73-fold) in OZ. One of the reasons for the microvascular dysfunction and hepatic injury after upregulation of iNOS might be due to the reaction of NO with  $O_2^-$  to form cytotoxic peroxynitrite and other reactive oxygen species [27, 51]. Peroxynitrite reduces the NO bioavailability for vasodilatation [52, 53]. Furthermore, peroxynitrite can modify cellular macromolecules and may aggravate adenosine triphosphate depletion, leading to hepatocyte and endothelial cell necrosis [54, 55] (Fig. 4). McNaughton et al. (2002) showed that in human cirrhotic livers, there was a significant increase in iNOS in the cirrhotic areas [56]. Li and Billiar (1999) reported that suppression of iNOS could represent a therapeutic strategy to prevent liver damage, as upregulation of iNOS expression appears to involve the coproduction of reactive oxygen species [57]. Therefore, selective inhibition of iNOS could be a possible strategy to reduce vasoconstriction and the resulting tissue damage and formation of necrosis, as observed in the OZ.

This strategy may not only be promising for hepatic outflow obstruction, but also also in other liver diseases. Hazam et al. observed a significant positive correlation between iNOS and eNOS levels compared with the severity of disease parameters of HEV-related acute hepatitis in a study population. In addition, they found that high levels of iNOS and eNOS were associated with an increased risk of HEV-related acute hepatitis and liver failure [58]. Tache et al. showed that infection with hepatitis B and C viruses induces iNOS expression in hepatocytes, suggesting that NO overproduction might have an important role in progression of chronic viral hepatitis to cirrhosis [59]. Based on the evaluation of 168 publications, Iwakiri and Kim describe in their review the significance of nitric oxide in various clinical liver diseases as fatty liver disease, viral hepatitis and hepatic fibrosis [60]. Thus, the investigation of iNOS seems to be important



not only for our model, but also for various other clinical liver diseases.

**Arachidonic acid pathway**

Activation of the arachidonic acid pathway can cause either vasodilatation or vasoconstriction. Upon activation of the arachidonic acid pathway, arachidonic acid is released from the cell membrane by the enzyme phospholipase A2 (Pla2g4a). The free arachidonic acid undergoes oxidation by Ptgs1 or Ptgs2 to prostaglandin G<sub>2</sub> and further to prostaglandin H<sub>2</sub>. In endothelial cells, prostaglandin H<sub>2</sub> is converted into prostacyclin by Ptgis and acts as a vasodilator. In contrast, prostaglandin H<sub>2</sub> is metabolized into thromboxane by Tbxas1 in Kupffer cells. Thromboxane binds to Tbxar and acts as a vasoconstrictor.

We selected 6 genes as marker genes: Pla2g4a, Ptgs1, Ptgs2, Ptgis, Tbxas1, and Tbxar (Fig. 1).

In this study, the genes associated with vasoconstriction such as Ptgs2 and Tbxas1 were upregulated in BZ and OZ at 24 h and 48 h post-op. Ptgs2 was the second highest upregulated vasoactive gene in OZ at 24 h post-op. This upregulation of Ptgs2 mRNA expression

corresponds to the observations published by Mohammed et al. (2004) and Schmedtje et al. (1997) [61, 62]. They also reported that the gene expression of Ptgs2 was induced after hepatic injury. Ptgs2 and thromboxane upregulation promote vasoconstriction in the presence of peroxynitrite, which is produced depending on NO-levels [62, 63] (Fig. 4).

Therefore, inhibition of iNOS could be an interesting strategy to reduce the detrimental vasoconstriction mediated by Ptgs2 and thromboxane.

**Endothelin pathway**

Activation of the endothelin pathway can also result in both: vasodilatation and vasoconstriction. Endothelin is synthesized and released by smooth muscle cells, endothelial cells, and Ito cells. The isoforms ET-1, ET-2, and ET-3 can bind to the ET receptors type A or B (1/2). In the liver, ET causes vasoconstriction by binding to ET-A receptors on perisinusoidal Ito cells or by binding to ET-B2 receptors on endothelial cells and Kupffer cells. In contrast, the binding of ET to the ETB1 receptor stimulates the endothelium to produce and release

prostacyclin. It also activates eNOS and causes vasodilatation by releasing NO [65–67].

We selected 3 genes as marker genes: Edn1, ET-R<sub>A</sub>, and ET-R<sub>B</sub> (Fig. 1).

In this study, ET-R<sub>A</sub> and Edn1 promoting vasoconstriction were upregulated in OZ. Edn1 was the third highest upregulated vasoactive gene in OZ. The upregulation of Edn1 corresponds to the findings of Earley et al. (2002), who observed that NO also causes an increased release of Edn1. Other studies have shown that Edn1 leads to a decrease in sinusoidal volumetric flow by vasoconstriction [68–70]. In addition, Edn1 increases the production of peroxynitrite [71] (Fig. 4).

Altogether, this suggests that inhibition of iNOS-expression could also lead to a reduction of vasoconstriction by Edn1.

### Druggable signal transduction pathways

Overproduction of vasoconstrictors and impairment of vasodilatation may lead to an imbalance in hepatic hemodynamics. The study of Liang et al. (2003) reported that microcirculatory injury in small-for-size liver grafts resulted in upregulation of mRNA expression of Edn1 (2.5- to sixfold) and iNOS (6.4- to 24-fold) [72]. Furthermore, they showed that the upregulation of Edn1 and iNOS leads to a deterioration of intracellular homeostasis.

Imbalance in hepatic hemodynamics may promote hepatic damage. The imbalances between vasoconstrictors (mainly induced by upregulation of Edn1 and cyclooxygenase-derived prostaglandins) and impaired vasodilation (mainly NO) are responsible for the increased vascular tone in the sinusoidal and postsinusoidal space, vasoconstriction and narrowing of the sinusoidal lumen, compromising blood flow, tissue oxygenation, and cell trafficking. Also, these imbalances together with

the increased intrahepatic resistance are important for the pathophysiology of portal hypertension in cirrhotic livers [23, 73].

As mentioned before, modulation of NO pathway by the non-specific NOS-inhibitor L-NAME impaired hepatic microcirculation and aggravated parenchymal damage after extended liver resection [26]. L-NAME leads to feedback regulation of NO expression and an increase of iNOS. The feedback regulation is followed by inhibition of eNOS and nNOS mediated by L-NAME. By inhibiting the eNOS and nNOS, the NO level may decrease. The decrease in NO level leads to transcription factor nuclear factor kB (NF-kB) activation. NF-kB, a key factor in iNOS expression, increased iNOS expression [55, 74, 75]. This could possibly explain that L-NAME impaired hepatic microcirculation and aggravated parenchymal damage after extensive liver resection. Therefore, modulation of iNOS should be investigated instead of using a non-specific modulation of the NO pathway as pursued before.

These considerations suggest in particular that the specific inhibition of iNOS expression could be a promising strategy to reduce liver damage after extensive liver resection. It appears that high NO levels due to the elevated iNOS expression lead to vasoregulatory imbalance and an increase of hepatic damage. This has already been investigated in other studies (Table 3). The administration of specific iNOS inhibitors such as Aminoguanidine, ONO-1714, Sivelestat, and 1400 W showed improvements in liver injury in experimental studies of ischemia-reperfusion and PHx [76–83]. Other strategies to modulate iNOS include expression control methods, e.g., using microRNAs or antisense RNA. There are interesting studies on the application of microRNAs or antisense RNA for instance in inflammatory livers or hepatocytes [84, 85]. In view of these publications, we speculate that

**Table 3** Examples of studies on the regulation of iNOS in the liver

Drug	Treatment	Species	Result	References
Aminoguanidine	Phx	rat	Decreased iNOS protein level	[75]
	LPS	rat	Attenuated LPS-induced hepatotoxicity	[76]
ONO-1714	Phx	pig	Reduced liver damage	[77]
	I/R	pig	Reduced liver ischemia-reperfusion damage	[78]
	I/R	pig	Reduced liver damage & stabilized hemodynamics	[79]
Sivelestat	I/R	rat	Prevented hepatic I/R injury	[80]
1400 W	transplantation	rat	Effective therapy for primary nonfunction of fatty liver grafts	[81]
	I/R	rat	Decreased NO metabolites level in serum	[82]
	ICC	tissue / cell	Suppressed cell proliferation, invasion, and migration in ICC	[83]
microRNA149	LPS	mice	Reduced inflammation in liver	[84]
asRNA	–	HC rat	Reduced iNOS mRNA levels	[85]

asRNAs Antisense RNA; HC Hepatocytes cells, I/R Ischemia-reperfusion, Phx Partial hepatectomy, ICC Intrahepatic cholangiocarcinoma

modulation of the NO signaling pathway by specific inhibition of iNOS expression could be a possible signal transduction pathway to also reduce liver damage due to outflow obstruction after extended liver resection. In the next study, we will further investigate the effect of iNOS and the downregulation of iNOS in our model.

## Conclusion

In our study, the NO pathway turned out to be the most affected pathway from the four investigated vasoactive pathways. Due to the central role of iNOS in the intermingled vasoactive pathways, selective downregulation of iNOS-expression seems to be the most promising approach to reduce the risk of post-operative liver failure.

## Abbreviations

BZ: Border zone; CT: Cycle threshold; cGMP: Cyclic guanosine monophosphate; DEGs: Differentially expressed genes; FHO: Focal hepatic outflow obstruction; HARR: Hepatic arterial buffer response; LEMming: Linear error model—ming; LIMMA: Linear models for microarray data; L-NAME: N( $\omega$ )-nitro-L-arginine methyl ester; NO: Nitric oxide; NOS: NO synthase; NZ: Normal zone; OZ: Outflow obstruction zone; PCA: Principal component analysis; PHx: Partial hepatectomy; RIN: RNA integrity number; RT-qPCR: Quantitative reverse transcription PCR; RMHVL: Right median hepatic vein ligation.

## Supplementary Information

The online version contains supplementary material available at <https://doi.org/10.1186/s12920-022-01364-z>.

**Additional file 1:** List of gene primers.

**Additional file 2:** List of all normalized gene expression data.

## Acknowledgements

This study was supported by the German Federal Ministry for Education and Research (BMBF) Virtual Liver Network.

## Author contributions

Conceptualization: J.A., S.V., U.D., O.D. Methodology: J.A., S.V., U.D. Software: S.V., R.F., M.T., U.D. Validation: J.A., S.V. Formal Analysis: J.A., S.V., U.D. Investigation: J.A. Resources: J.A. Data Curation: J.A., U.D. Writing – Original Draft Preparation: J.A., U.D. Writing – Review & Editing: J.A., S.V., R.F., M.T., U.S., U.D., O.D. Visualization: J.A., S.V. Supervision: U.S., U.D., Project Administration: U.D. Funding Acquisition: U.D. All authors read and approved by the final manuscript.

## Funding

Open Access funding enabled and organized by Projekt DEAL. This study was supported by German Federal Ministry for Education and Research (BMBF) Virtual Liver Network (grant numbers 0315765 (UK Jena)).

## Availability of data and materials

All data generated or analysed during this study are included in this published article and its Additional information files.

## Declarations

### Ethics approval and consent to participate

All procedures, experiments, and housing of the animals were carried out according to current German regulations and guidelines for animal welfare and to international principles of laboratory animal care, following the ARRIVE Guidelines Checklist as well. Ethics committee of Thüringer Landesamt für

Verbraucherschutz, Thuringia, Germany, approved this animal study. The protocols were approved by the Thüringer Landesamt für Verbraucherschutz, Thuringia, Germany (Approval-Number: 02–023/14).

### Consent for publication

Not applicable.

### Competing interests

The authors declare that they have no competing interests.

### Author details

<sup>1</sup>Experimental Transplantation Surgery, Department of General, Visceral and Vascular Surgery, Jena University Hospital, Drackendorfer Str. 1, 07747 Jena, Germany. <sup>2</sup>Leibniz Institute for Natural Product Research and Infection Biology Hans Knöll Institute (HKI), Beutenbergstraße 11a, 07745 Jena, Germany. <sup>3</sup>Institute for System Dynamics, University of Stuttgart, Pfaffenwaldring 9, 70569 Stuttgart, Germany. <sup>4</sup>Dr. Magarete Fischer-Bosch Institute for Clinical Pharmacology, Auerbachstr. 112, 70376 Stuttgart, Germany. <sup>5</sup>Department of General, Visceral and Vascular Surgery, Jena University Hospital, Erlanger Allee 101, 07747 Jena, Germany. <sup>6</sup>Institute of Pathology, Jena University Hospital, Ziegelmühlenweg 1, 07743 Jena, Germany.

Received: 14 January 2022 Accepted: 21 September 2022

Published online: 07 October 2022

## References

- Benoit JN, Womack WA, Hernandez L, Granger DN. "Forward" and "backward" flow mechanisms of portal hypertension: relative contributions in the rat model of portal vein stenosis. *Gastroenterology*. 1985;89(5):1092–6.
- Henderson, J.M. Portal Hypertension, bock gastrointestinal surgery, Section 3, chapter 12. <https://de.scribd.com/document/181940159/9780723430698.pdf> (2015).
- Dirsch O, et al. Recovery of liver perfusion after focal outflow obstruction and liver resection. *Transplantation*. 2008;85(5):748–56.
- Huang H, et al. Hepatic arterial perfusion is essential for the spontaneous recovery from focal hepatic venous outflow obstruction in rats. *Am J Transplant*. 2011;11(11):2342–52.
- Merion RM, Burtch GD, Ham JM, Turcotte JG, Campbell DA. The hepatic artery in liver transplantation. *Transplantation*. 1989;48(3):438–43.
- Fan ST The middle hepatic vein controversy. In: Fan ST, editor. *Living donor liver transplantation*. Hong Kong: Takunpao Publishing Co., Ltd. p. 75–88 (2008).
- Kiuchi T, et al. Impact of graft size mismatching on graft prognosis in liver transplantation from living donors 1, 2. *Transplantation*. 1999;67(2):321–7.
- Ikegami T, et al. Small-for-size graft, small-for-size syndrome and inflow modulation in living donor liver transplantation. *J Hepatobiliary Pancreat Sci*. 2020;27(11):799–809.
- Greenbaum LE, Ukomadu C, Tchorz JS. Clinical translation of liver regeneration therapies: a conceptual road map. *Biochem Pharmacol*. 2020;175:113847.
- Ikegami T et al Application of splenectomy to decompress portal pressure in left lobe living donor liver transplantation. *Fukuoka igaku zasshi=Hukuoka acta medica*. (2013); 104(9), 282–289.
- Ikegami T, et al. Strategies for successful left-lobe living donor liver transplantation in 250 consecutive adult cases in a single center. *J Am Coll Surg*. 2013;216(3):353–62.
- Watanabe Y, et al. Significance of laparoscopic splenectomy in patients with hypersplenism. *World J Surg*. 2007;31(3):549–55.
- Winslow ER, Brunt LM. Perioperative outcomes of laparoscopic versus open splenectomy: a meta-analysis with an emphasis on complications. *Surgery*. 2003;134(4):647–53.
- Bosch J, Iwakiri Y. The portal hypertension syndrome: etiology, classification, relevance, and animal models. *Hep Intl*. 2018;12(1):1–10.
- Bari K, Garcia-Tsao G. Treatment of portal hypertension. *World J Gastroenterol: WJG*. 2012;18(11):1166.
- Dell'Era A, De Franchis R, Iannuzzi F. Acute variceal bleeding: pharmacological treatment and primary/secondary prophylaxis. *Best Pract Res Clin Gastroenterol*. 2008;22(2):279–94.

17. Nair H, Berzigotti A, Bosch J. Emerging therapies for portal hypertension in cirrhosis. *Expert Opin Emerg Drugs*. 2016;21(2):167–81.
18. Mauro E, Gadano A. What's new in portal hypertension? *Liver Int*. 2020;40:122–7.
19. Fausto N, Campbell JS, Riehle KJ. Liver regeneration. *Hepatology*. 2006;43(S1):S45–53.
20. Lauth W W Mechanism and role of intrinsic regulation of hepatic arterial blood flow: hepatic arterial buffer response. *Am J Phys-Gastrointest Liver Physiol*. (1985); 249(5), 549–556.
21. Michalopoulos GK. Liver regeneration. *J Cell Physiol*. 2007;213(2):286–300.
22. Reynaert H, Thompson MG, Thomas T, Geerts A. Hepatic stellate cells: role in microcirculation and pathophysiology of portal hypertension. *Gut*. 2002;50(4):571–81.
23. Vollmar B, Menger MD. The hepatic microcirculation: mechanistic contributions and therapeutic targets in liver injury and repair. *Physiol Rev*. 2009;89(4):1269–339.
24. Riddiough GE, Fifis T, Muralidharan V, Perini MV, Christophi C. Searching for the link; mechanisms underlying liver regeneration and recurrence of colorectal liver metastasis post partial hepatectomy. *J Gastroenterol Hepatol*. 2019;34(8):1276–86.
25. Riddiough G E, Jalal Q, Perini MV, & Majeed A W Liver regeneration and liver metastasis. In *Seminars in cancer biology* 71, 86–97 (2021). Academic Press.
26. Huang H, et al. Reduced hepatic arterial perfusion impairs the recovery from focal hepatic venous outflow obstruction in liver-resected rats. *Transplantation*. 2014;97(10):1009–18.
27. Alexander B. The role of nitric oxide in hepatic metabolism. *Nutrition*. 1998;14(4):376–90.
28. Cantré D, et al. Nitric oxide reduces organ injury and enhances regeneration of reduced-size livers by increasing hepatic arterial flow. *J British Surg*. 2008;95(6):785–92.
29. Arlt J, et al. Modulation of hepatic perfusion did not improve recovery from hepatic outflow obstruction. *BMC Pharmacol Toxicol*. 2017;18(1):1–13.
30. Feuer R, et al. LEMming: a linear error model to normalize parallel quantitative real-time PCR (qPCR) data as an alternative to reference gene based methods. *PLoS ONE*. 2015;10(9): e0135852.
31. Team R C R: A language and environment for statistical computing. 2013.
32. Warnes GR, et al. gplots: various R programming tools for plotting data. R package version. 2016;3:1.
33. Abdi H, Williams LJ. Principal component analysis. *Wiley Interdisciplinary Rev Comput Stat*. 2010;2(4):433–59.
34. Ritchie ME, et al. limma powers differential expression analyses for RNA-sequencing and microarray studies. *Nucleic Acids Res*. 2015;43(7):e47–e47.
35. Kim YM, Talanian RV, Billiar TR. Nitric oxide inhibits apoptosis by preventing increases in caspase-3-like activity via two distinct mechanisms. *J Biol Chem*. 1997;272(49):31138–48.
36. Rockey D C Hepatic blood flow regulation by stellate cells in normal and injured liver. In *seminars in liver disease* 21(3), pp. 337–350 (2001). Copyright© 2001 by Thieme Medical Publishers, Inc., 333 Seventh Avenue, New York, NY 10001, USA. Tel.:+ 1 (212) 584–4662
37. Clemens M G, & Zhang J X Regulation of sinusoidal perfusion: in vivo methodology and control by endothelins. In *seminars in liver disease* 19(4), 383–396. (1999) © 1999 by Thieme Medical Publishers, Inc.
38. Fernández M, et al. Angiogenesis in liver disease. *J Hepatol*. 2009;50(3):604–20.
39. Lee JS, Semela D, Iredale J, Shah VH. Sinusoidal remodeling and angiogenesis: a new function for the liver-specific pericyte? *Hepatology*. 2007;45(3):817–25.
40. Theocharis SE, Skopelitou AS, Margeli AP, Pavlaki KJ, Kittas C. Proliferating cell nuclear antigen (PCNA) expression in regenerating rat liver after partial hepatectomy. *Dig Dis Sci*. 1994;39(2):245–52.
41. Carreras CW, Santi DV. The catalytic mechanism and structure of thymidylate synthase. *Annu Rev Biochem*. 1995;64(1):721–62.
42. Kowalczyk A, Kleniewska P, Kolodziejczyk M, Skibska B, Goraca A. The role of endothelin-1 and endothelin receptor antagonists in inflammatory response and sepsis. *Arch Immunol Ther Exp*. 2015;63(1):41–52.
43. Martin-Sanz P, et al. Nitric oxide in liver inflammation and regeneration. *Metab Brain Dis*. 2002;17(4):325–34.
44. Dold S, et al. Portal hyperperfusion after extended hepatectomy does not induce a hepatic arterial buffer response (HABR) but impairs mitochondrial redox state and hepatocellular oxygenation. *PLoS ONE*. 2015;10(11): e0141877.
45. Audebert C, Bekheit M, Bucur P, Vibert E, Vignon-Clementel IE. Partial hepatectomy hemodynamics changes: Experimental data explained by closed-loop lumped modeling. *J Biomech*. 2017;50:202–8.
46. Ma XL, et al. Expression of inducible nitric oxide synthase in the liver is under the control of nuclear factor kappa B in concanavalin A-induced hepatitis. *J Gastroenterol Hepatol*. 2008;23(7pt2):231–5.
47. Morishita T, et al. Vasculoprotective roles of neuronal nitric oxide synthase. *FASEB J*. 2002;16(14):1994–6.
48. Carnovale CE, Ronco MT. Role of nitric oxide in liver regeneration. *Ann Hepatol*. 2012;11(5):636–47.
49. Eum HA, Park SW, Lee SM. Role of nitric oxide in the expression of hepatic vascular stress genes in response to sepsis. *Nitric Oxide*. 2007;17(3–4):126–33.
50. Pfeilschifter J, Eberhardt W, Beck KF. Regulation of gene expression by nitric oxide. *Pflugers Arch*. 2001;442(4):479–86.
51. Boyer-Diaz Z, et al. Oxidative stress in chronic liver disease and portal hypertension: potential of DHA as nutraceutical. *Nutrients*. 2020;12(9):2627.
52. Beckman JS, Koppenol WH. Nitric oxide, superoxide, and peroxynitrite: the good, the bad, and ugly. *Am J Physiol Cell Physiol*. 1996;271(5):C1424–37.
53. Stamler JS, Singel DJ, Loscalzo J. Biochemistry of nitric oxide and its redox-activated forms. *Science*. 1992;258(5090):1898–902.
54. Jaeschke H, Knight TR, Bajt ML. The role of oxidant stress and reactive nitrogen species in acetaminophen hepatotoxicity. *Toxicol Lett*. 2003;144(3):279–88.
55. Kopincová J, Púžserová A, Bernátová I. L-NAME in the cardiovascular system—nitric oxide synthase activator? *Pharmacol Rep*. 2012;64(3):511–20.
56. McNaughton L, et al. Distribution of nitric oxide synthase in normal and cirrhotic human liver. *Proc Natl Acad Sci*. 2002;99(26):17161–6.
57. Li J, Billiar TR. Determinants of nitric oxide protection and toxicity in liver. *Am J Physiol-Gastrointest Liver Physiol*. 1999;276(5):1069–73.
58. Hazam RK, Deka M, Kar P. Role of nitric oxide synthase genes in hepatitis E virus infection. *J Viral Hepatitis*. 2014;21(9):671–9.
59. Tache DE, et al. Inducible nitric oxide synthase expression (iNOS) in chronic viral hepatitis and its correlation with liver fibrosis. *Rom J Morphol Embryol*. 2014;55(Suppl 2):S539–43.
60. Iwakiri Y, Kim MY. Nitric oxide in liver diseases. *Trends Pharmacol Sci*. 2015;36(8):524–36.
61. Mohammed NA, El-Hafiz HA, McMahon RFT. Distribution of constitutive (COX-1) and inducible (COX-2) cyclooxygenase in postviral human liver cirrhosis: a possible role for COX-2 in the pathogenesis of liver cirrhosis. *J Clin Pathol*. 2004;57(4):350–4.
62. Schmedtje JF, Ji YS, Liu WL, DuBois RN, Runge MS. Hypoxia induces cyclooxygenase-2 via the NF- $\kappa$ B p65 transcription factor in human vascular endothelial cells. *J Biol Chem*. 1997;272(1):601–8.
63. Cooke CLM, Davidge ST. Peroxynitrite increases iNOS through NF- $\kappa$ B and decreases prostacyclin synthase in endothelial cells. *Am J Physiol Cell Physiol*. 2002;282(2):C395–402.
64. Zou MH, Ullrich V. Peroxynitrite formed by simultaneous generation of nitric oxide and superoxide selectively inhibits bovine aortic prostacyclin synthase. *FEBS Lett*. 1996;382(1–2):101–4.
65. Bauer M, et al. Functional significance of endothelin B receptors in mediating sinusoidal and extrasinusoidal effects of endothelins in the intact rat liver. *Hepatology*. 2000;31(4):937–47.
66. Clozel M, Gray GA, Breu V, Löffler BM, Osterwalder R. The endothelin ETB receptor mediates both vasodilation and vasoconstriction in vivo. *Biochem Biophys Res Commun*. 1992;186(2):867–73.
67. Higuchi H, Satoh T. Endothelin-1 induces vasoconstriction and nitric oxide release via endothelin ETB receptors in isolated perfused rat liver. *Eur J Pharmacol*. 1997;328(2–3):175–82.
68. Earley S, Nelin LD, Chicoine LG, Walker BR. Hypoxia-induced pulmonary endothelin-1 expression is unaltered by nitric oxide. *J Appl Physiol*. 2002;92(3):1152–8.
69. Garcia-Pagán JC, Zhang JX, Sonin N, Nakanishi K, Clemens MG. Ischemia/reperfusion induces an increase in the hepatic portal vasoconstrictive response to endothelin-1. *Shock (Augusta Ga)*. 1999;11(5):325–9.

70. Pannen BH, Bauer MICHAEL, Zhang JX, Robotham JL, Clemens MG. Endotoxin pretreatment enhances portal venous contractile response to endothelin-1. *Am J Physiol-Heart Circ Physiol.* 1996;270(1):H7–15.
71. Galle J, Lehmann-Bodem C, Hübner U, Heinloth A, Wanner C. CyA and OxLDL cause endothelial dysfunction in isolated arteries through endothelin-mediated stimulation of O<sub>2</sub>– formation. *Nephrol Dial Transplant.* 2000;15(3):339–46.
72. Liang TB, et al. Distinct intragraft response pattern in relation to graft size in liver transplantation. *Transplantation.* 2003;75(5):673–8.
73. Shah V. Molecular mechanisms of increased intrahepatic resistance in portal hypertension. *J Clin Gastroenterol.* 2007;41:S259–61.
74. Miller MJS, et al. Failure of L-NAME to cause inhibition of nitric oxide synthesis: role of inducible nitric oxide synthase. *Inflamm Res.* 1996;45(6):272–6.
75. Carnovale CE, et al. Nitric oxide release and enhancement of lipid peroxidation in regenerating rat liver. *J Hepatol.* 2000;32(5):798–804.
76. Beheshti F, et al. Protective effect of aminoguanidine against lipopolysaccharide-induced hepatotoxicity and liver dysfunction in rat. *Drug Chem Toxicol.* 2021;44(2):215–21.
77. Kukita K, et al. Remnant liver injury after hepatectomy with the pringle maneuver and its inhibition by an iNOS inhibitor (ONO-1714) in a pig model. *J Surg Res.* 2005;125(1):78–87.
78. Meguro M, et al. A novel inhibitor of inducible nitric oxide synthase (ONO-1714) prevents critical warm ischemia-reperfusion injury in the pig liver. *Transplantation.* 2002;73(9):1439–46.
79. Meguro M, et al. Apoptosis and necrosis after warm ischemia-reperfusion injury of the pig liver and their inhibition by ONO-1714. *Transplantation.* 2003;75(5):703–10.
80. Nakano Y, et al. Prevention of leukocyte activation by the neutrophil elastase inhibitor, sivelestat, in the hepatic microcirculation after ischemia-reperfusion. *J Surg Res.* 2009;155(2):311–7.
81. Liu Q, et al. Role of inducible nitric oxide synthase in mitochondrial depolarization and graft injury after transplantation of fatty livers. *Free Radical Biol Med.* 2012;53(2):250–9.
82. Chen TH, Liao FT, Yang YC, Wang JJ. Inhibition of inducible nitric oxide synthesis ameliorates liver ischemia and reperfusion injury induced transient increase in arterial stiffness. *Trans Proc.* 2014;46(4):1112–6.
83. Liu S, et al. iNOS is associated with tumorigenicity as an independent prognosticator in human intrahepatic cholangiocarcinoma. *Cancer Manage Res.* 2019;11:8005.
84. Zhang Q, et al. MicroRNA-149\* suppresses hepatic inflammatory response through antagonizing STAT3 signaling pathway. *Oncotarget.* 2017;8(39):65397.
85. Yoshigai E, et al. Natural antisense transcript-targeted regulation of inducible nitric oxide synthase mRNA levels. *Nitric Oxide.* 2013;30:9–16.

## Publisher's Note

Springer Nature remains neutral with regard to jurisdictional claims in published maps and institutional affiliations.

Ready to submit your research? Choose BMC and benefit from:

- fast, convenient online submission
- thorough peer review by experienced researchers in your field
- rapid publication on acceptance
- support for research data, including large and complex data types
- gold Open Access which fosters wider collaboration and increased citations
- maximum visibility for your research: over 100M website views per year

At BMC, research is always in progress.

Learn more [biomedcentral.com/submissions](https://biomedcentral.com/submissions)

